Multiscale Analysis of Panel Gaps in a Large Parabolic Reflector

Nader Farahat* and Raj Mittra**
*Polytechnic University of Puerto Rico
P.O. box 192017 San Juan, PR 00919
**The Pennsylvania State University, 319 EE East
University Park, PA, 16802, USA

Abstract

The effect of the gaps between the panels of a reflector, used as a radio-telescope, is analyzed in this paper via the multiscale and array factor approach. Initially, the simulation is carried out by numerical integration as well as the Finite Difference Time Domain (FDTD) Method for a reflector with a moderately large diameter, and the results are then scaled for the actual size, which is thousands of wavelengths in diameter in the frequency range of interest. The array factor concept is employed to demonstrate the fact that the grating lobe cannot arise for the typical gap size of the reflector.

Multiscale approach

We investigate a large reflector antenna, which is a 120 ft (36.57 m) diameter radio-telescope, originally designed for operation up to 10 GHz, but now being considered for application at higher frequencies. However, in higher frequencies the quasi-periodic structure of the gaps in the reflector might cause grating lobes in the far-field pattern. The gaps consist of the hollow rings and strips dividing the panels similar to the Fig. 1. The width of the gaps is one wavelength (in the frequency of interest) whereas the length of the panels is in order of 1000 wavelengths. The diameter of the main parabolic reflector is on the order of 10,000 wavelengths, which makes it impractical for the direct numerical simulation. Therefore we use a multiscale approach to study the grating lobes.

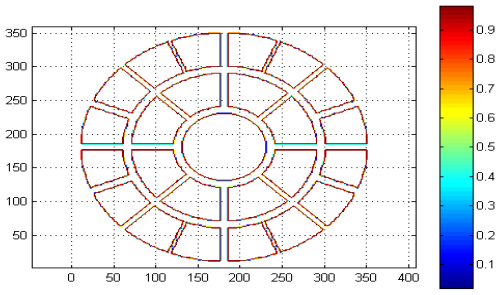

Fig.1. Illustration of circular reflector (diameter 34 lambda); panels (5 lambda) and gap width 1 lambda; x and y axes show the cell numbers.

To estimate the level of the grating lobes, first we compute the far-field pattern due to the circular aperture of 34 wavelength diameter with the gaps of one wavelength (where the surface current is set to zero in the shadow of the gaps in the aperture) between the 5-wavelength long panels shown in Fig. 1. In this approach (shadowing) the assumption is that the current is uniformly distributed on the panels. The H- and E-plane far-filed patterns of the circular aperture (solid panel) vs. slotted (with panels) are shown in Figs. 2 and 3, respectively. It is seen that the first grating lobe arises around 10 degrees.

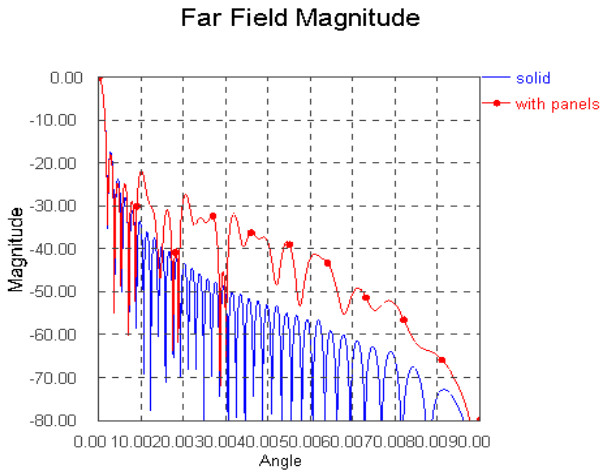

Fig.2. H-plane far-field pattern of circular aperture with and without panels with diameter of 34 lambda (shadowing approach).

In the next step to validate the shadowing approach we compute the scattered far-field of the same size flat circular reflector with and without the gaps, illuminated by a normally incident plane wave using the Finite Difference Time Domain (FDTD) Method [1]. The scattered-field formulation of the FDTD Method is used to simulate the flat reflector [2]. The normally incident wave is analytically introduced everywhere in the computational domain particularly on the surface of the perfect electric conductor of the reflector. Next the scattered field is computed throughout the domain by setting the tangential components of scattered electric fields to

negative of those of incident field on the surface of the reflector. Upon the completion of the simulation the equivalent surface currents at the frequency of interest on the Huygens box surrounding the reflector, which was stored throughout the simulation is used to compute the scattered far-field pattern via the near-to-far-field transformation.

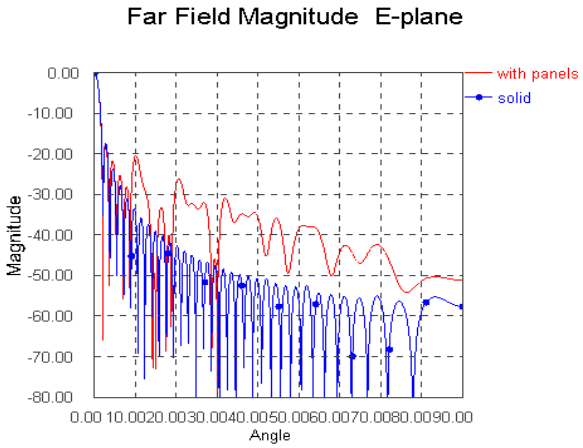

Fig.3. E-plane far-field pattern of circular aperture with and without panels with diameter of 34 lambda (shadowing approach).

The comparison of the patterns for the solid panels in both H- and E-planes using the two methods, presented in Figs. 4 and 5, respectively, shows that the difference is limited to the far-end lobes. This is due to the fact that in the shadowing approach the edge diffraction is ignored. The same comparison is shown in Figs. 6 and 7 for the slotted case using these two methods. Once again, the difference is limited to the far-end lobes. One can conclude that the diffraction effect due to the gaps is insignificant and that the shadowing approach predicts the level of the grating lobes adequately.

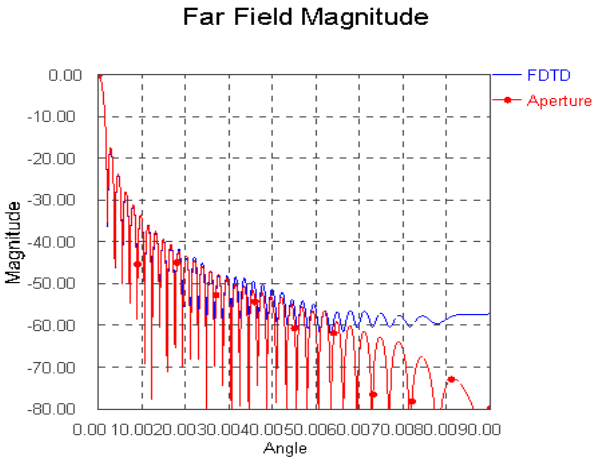

Fig.4. H-plane far-field pattern of solid circular disc with diameter of 34 lambda.

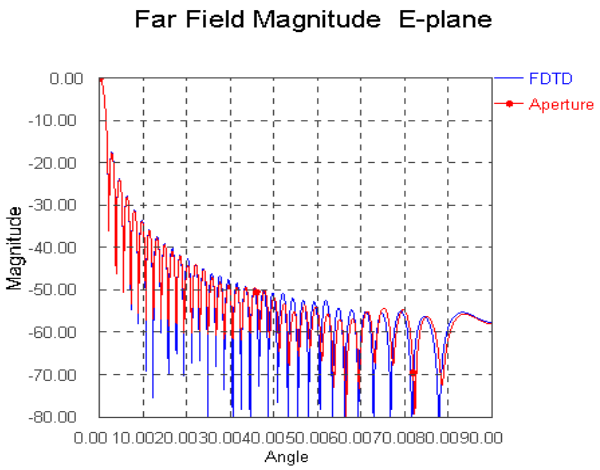

Fig.5. E-plane far-field pattern of solid circular disc with diameter of 34 lambda.

Based on the above simulation we can predict the pattern of the slotted reflector simply by arraying the panels with uniform current distributions. The grating lobes level and the locations depend on the length of each element and the inter-element separation. Consequently, we use the array factor concept to predict the performance of the slotted reflector. For simplicity we consider only the linear array of panels.

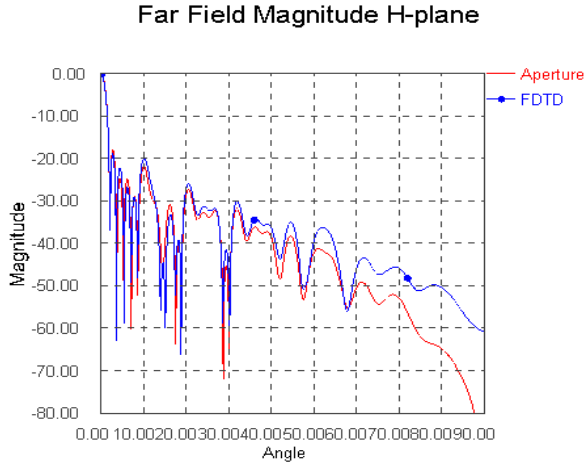

Fig.6. H-plane far-field pattern of circular reflector with diameter of 34 lambda with panels.

In the linear array of panels the grating lobe levels and locations depend on a, the length of each element and d, the inter-element separation, as shown in Fig. 8. At first we assume a linear array of 5 panels with a = 5λ, and d = 6λ (therefore the gap between the panels is g = λ). The pattern of the single element,

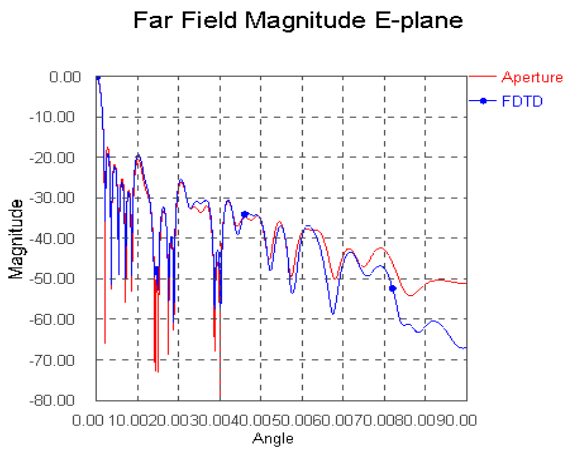

Fig.7. E-plane far-field pattern of circular reflector with diameter of 34 lambda with panels.

On the other hand, the array factor expression is given by [3] $AF = \dfrac{\sin(kNd\sin\theta/2)}{\sin(kd\sin\theta/2)}$, which has the first peak when $kd\sin\theta/2 = \pi$ hence $\theta_p = \sin^{-1}(1/d_\lambda) = \sin^{-1}(1/(a_\lambda + g_\lambda))$, where a_λ and g_λ are the electrical dimensions of the panel and gap respectively.

By comparing the expressions for the θ_p and θ_n, one can see that as long as the gap size is small compared to the length of the panel, the difference between these angles is insignificant. This is shown in Fig.10 for the array of 11 panels, with a length of 1170λ and a gap of λ. The difference between the two patterns is seen to be insignificant, for the reason given above.

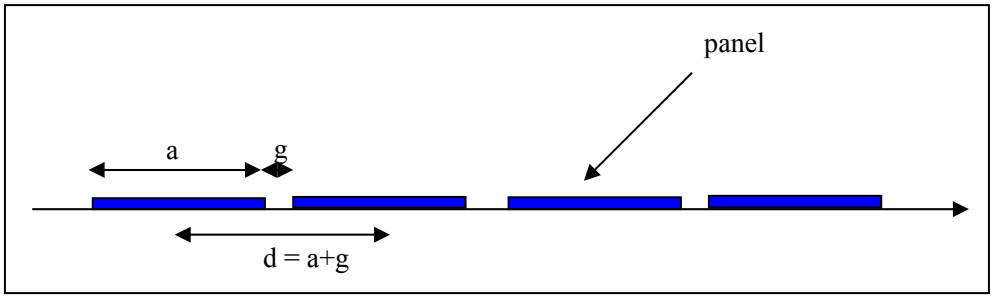

Fig.8. Illustration of linear array of N panels with length a and spacing d.

array factor, and pattern multiplication is shown in Fig. 9. The pattern multiplication is also compared by the pattern of the solid panels (a = 6λ, d = 6λ, and g = 0). The first grating lobe again shows up around 10 degrees (first peak angle θ_p) where the array factor has the grating lobe. However, it can be shown as the inter-element spacing is decreased (in other words when the gap becomes small compared to the panel size) the null of the single element pattern (first null angle θ_n) moves closer to the grating lobe of the array factor, and this, in turn, reduces the difference between the patterns of the solid and slotted panels.

The individual panel far-field pattern has the Sinc function form $E = \dfrac{\sin(ka\sin\theta/2)}{ka\sin\theta/2}$ and the first null occurs when the argument of the Sinc function is equal to π and, therefore, where a_λ is the electrical length of the panel.

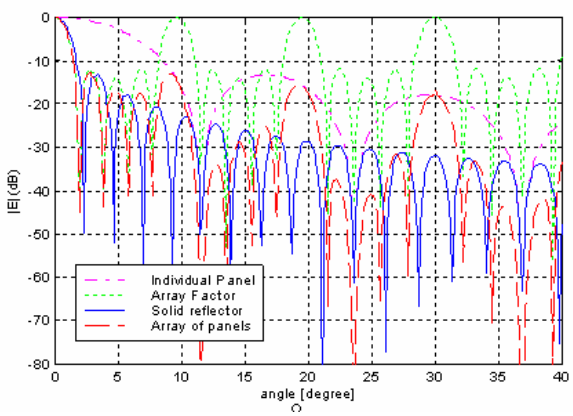

Fig.9. Far-field pattern of linear array of 5 panels (a = 5λ, d = 6λ, and g = λ).

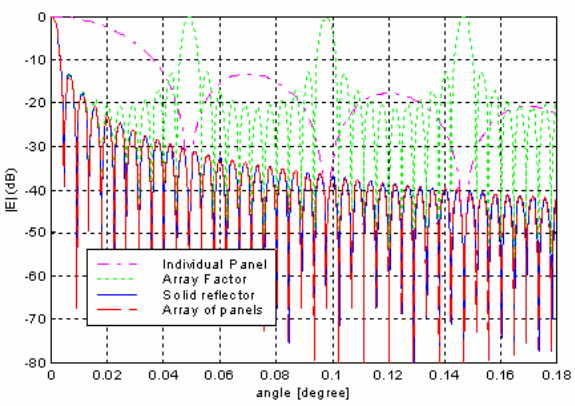

Fig.10. Far-field pattern of linear array of 11 panels (a = 1170λ, and g = λ).

References:

[1] K. S. Yee, "Numerical solution of initial boundary value problems involving Maxwell's equations in isotropic media," IEEE Trans. Antennas and Propagat., vol. AP-14, pp. 302-307, May 1966.

[2] A. Taflove and S. C. Hagness, Computational Electromangeics: The Finite-Difference Time-Domain Method, 2nd ed. Boston, MA: Artech, pp. 224-227, 2000.

[3] "Antenna Theory, Analysis and Design", C. A. Balanis, Second Edition, John Wiley & Sons, Inc. pp. 582–583, 1982.

Nader Farahat is Associate Professor in the Electrical Engineering Department of Polytechnic University of Puerto Rico. He is also adjunct research associate at Pennsylvania State University.

Raj Mittra is Professor in the Electrical Engineering Department of the Pennsylvania State University and the Director of the Electromagnetic Communication Laboratory. He is also the President of RM Associates, which is a consulting organization that provides services to industrial and governmental organizations, both in the U. S. and abroad.